Iran J Pathol. 2027;22(1):105–112 | ISSN 2345-3656 | MAIN SUBJECTS Endocrine Pathology

Descriptive Thyroid Histology after Intestinal Serosal Injury and Beclomethasone Exposure in 12- and 18-month-old Rats

Bekhruz Abdurakhmonovich Kibriev[1], **Mukhriddin Ochilovich Umbarov**[2*], **Rokhila Bakhriddinovna Mengliyeva**[2], **Navruzbek Allanazar o'g'li Ergashev**[3]

1. *Bukhara State Medical Institute named after Abu Ali ibn Sino, Bukhara, Uzbekistan*
2. *Department of Internal Medicine, Termez Branch of Tashkent State Medical University, Termez, Uzbekistan*
3. *Department of Surgical Sciences, Termez University of Economics and Service, Termez, Uzbekistan*

RECEIVED 09 Sep 2026 ACCEPTED 20 Oct 2026 PUBLISHED ONLINE 24 Oct 2026 DOI 10.22034/ijp.2026.2089875.3724

ABSTRACT

Background & Objective: To describe selected thyroid histological observations after combined intestinal serosal injury, postoperative recovery, repeated gavage, vehicle and beclomethasone exposure in 12- and 18-month-old rats.

Methods: Seventy male outbred albino rats were allocated to intact-control (10 per age) or combined-exposure groups (25 per age). Experimental animals underwent ileal serosal abrasion followed by beclomethasone dipropionate gavage (0.05 mg/kg daily for 14 days from postoperative day 14). Six animals died before dosing; 64 survived. This exploratory analysis transcribed archived dissertation summaries and recalculated fractions from pooled selected-ROI Ki-67 counts without new image analysis or recoverable animal-level linkage.

Results: Reported follicular diameters were 66.2 versus 66.7 µm at 12 months and 67.3 versus 69.1 µm at 18 months (control versus combined exposure). Selected-region Van Gieson-positive areas were 16.2% versus 36.8% and 21.4% versus 38.8%; Alcian blue-positive areas were 4.6% versus 14.5% and 4.7% versus 13.6%. Archived pooled selected-ROI Ki-67 counts were 42/263 versus 4/55 and 30/173 versus 4/47 (positive/total), with undocumented numbers of contributing images, sections and animals.

Conclusion: Archived summaries document higher stain-positive area percentages in selected experimental regions alongside small numerical differences in follicular dimensions. These observations provide a descriptive basis for further study; undocumented sampling prevents animal-level inference or attribution to beclomethasone alone.

KEYWORDS Beclomethasone, Immunohistochemistry, Ki-67 Antigen, Rats, Thyroid Gland, Tissue Adhesions

Corresponding Information: Mukhriddin Ochilovich Umbarov, Department of Internal Medicine, Termez Branch of Tashkent State Medical University, Termez, Uzbekistan, mmmumbarovvv@gmail.com

Copyright © 2027 The Author(s). This is an open-access article distributed under the terms of the CC BY 4.0, which permits unrestricted use, distribution, and reproduction in any medium, provided the original work is properly cited.

INTRODUCTION

Glucocorticoid exposure can alter thyroid regulation, but endocrine and structural outcomes should be evaluated separately. Wilber and Utiger demonstrated suppression of circulating thyroid-stimulating hormone after glucocorticoid administration in humans and rats (1). Experimental work with dexamethasone has also examined histological, immunohistochemical and biochemical changes in the adult rat thyroid (2). These observations support studying the thyroid during glucocorticoid exposure without assuming that every morphological change represents clinically meaningful thyroid dysfunction. Human postmortem observations have also linked glucocorticoid treatment to reduced hypothalamic thyrotropin-releasing hormone messenger RNA expression (3). This central regulatory evidence does not, by itself, identify a direct toxic effect on thyroid follicular cells.

Intestinal adhesion formation provides a setting in which tissue injury, inflammation, repair and drug exposure coexist. Experimental studies have identified contributions from resident peritoneal macrophages and CD163-positive macrophage populations to postoperative adhesion development (4, 5). Consequently, thyroid findings obtained after an adhesion-induction procedure followed by anti-inflammatory treatment represent a response to several exposures. An intact control can establish a reference appearance, but it cannot separate the effects of surgery, adhesions and the administered drug. Mesothelial-cell lineage studies and experiments on calcium-dependent membrane bridges further implicate the injured mesothelial surface in adhesion initiation (6, 7). Neutrophil extracellular traps and their clearance by DNases have also been investigated in adhesion formation (8). These local mechanisms justify treating the surgical component as a distinct exposure in the present model.

A combined assessment of follicular structure, extracellular matrix staining and cellular labeling may describe tissue changes that are incompletely reflected by average follicular dimensions. Ki-67 expression is regulated across the cell cycle, and its abundance is not a simple binary measure of proliferative behavior (9, 10). Interpretation therefore requires attention to the cells counted, the sampled tissue compartment and the distinction between image-level observations and independent

animals. Experimental studies show that Ki-67 participates in heterochromatin organization and mitotic chromosome dispersion (11, 12). A staining fraction consequently reflects the sampled population and cell state, rather than a direct measure of gland function.

The present exploratory report describes archived thyroid morphometric summaries, selected-region staining areas and Ki-67 cell counts from a larger experimental project involving 12- and 18-month-old rats. Its purpose is to describe the retained observations after intestinal serosal injury and subsequent beclomethasone exposure, using intact controls as a baseline reference, and to identify the sampling information needed for confirmatory analysis.

METHODS

Study design and animals

This report uses the intact-control and adhesion-plus-glucocorticoid arms of a larger three-arm experiment involving 120 outbred albino rats aged 12 or 18 months. The parent experiment also included 50 animals receiving subsequent ginger treatment; those animals are outside the present analysis. The present analysis included 70 male rats obtained from the institution's vivarium, with 35 animals per age stratum: 10 intact controls and 25 experimental animals. Baseline body weights ranged from 280 to 350 g at 12 months and from 380 to 450 g at 18 months. Experimental procedures were conducted between May and July 2025.

Animals were acclimatized for 7 days before surgery at 22 ± 2°C and 55 ± 10% relative humidity under a 12-hour light/dark cycle, with ad libitum access to standard rodent chow and water. Entry assessment included general appearance, activity, food intake and body weight; animals with overt signs of illness were not included. Allocation to groups was performed using simple randomization.

Two experimental animals aged 12 months died on postoperative days (PODs) 3 and 5, and four aged 18 months died on PODs 2, 4, 6 and 8. All deaths preceded the first drug gavage on POD 14. Premortem observations included reduced locomotor activity and transient piloerection. Gross post-mortem inspection showed no intestinal perforation, suture dehiscence, mechanical bowel obstruction or generalized peritonitis. Early postoperative surgical stress and individual vulnerability were considered possible explanations; these observations did not establish a definitive cause of death. There were no control deaths and no other animals were excluded from the surviving cohorts. All 64 survivors completed the study and underwent histological and immunohistochemical evaluation: 10 controls and 23 experimental animals at 12 months, and 10 controls and 21 experimental animals at 18 months. Individual-animal tracking for specific quantitative endpoints remains unavailable. The timing excludes exposure to the administered drug as the cause of these deaths, but does not exclude survivor-selection bias in the remaining cohort.

The animal study was approved by the Ethics Committee of Bukhara State Medical Institute (protocol No. 46, dated 23 May 2025). Surgical procedures were undertaken using aseptic precautions. Reporting was assessed against the ARRIVE 2.0 guidelines and their explanation and elaboration (13, 14).

Adhesion model and drug administration

General anesthesia was induced by intraperitoneal ketamine (80 mg/kg) and xylazine (10 mg/kg). Postoperative analgesia consisted of buprenorphine (0.03 mg/kg, subcutaneously) every 12 hours for the first 48 hours.

Under aseptic conditions and general anesthesia, a midline laparotomy was performed. A 3-cm segment of distal ileum approximately 5 cm proximal to the ileocecal valve was exteriorized. Non-perforating serosal abrasion was produced using a sterile 2 × 2 cm cotton gauze pad, with 20 uniform back-and-forth strokes over a 2-cm longitudinal distance. A single experienced surgeon applied gentle, consistent manual pressure until uniform subserosal petechiae appeared, without perforation. Abrasion duration was not recorded separately; the procedure was standardized by the count of 20 back-and-forth strokes and the petechial endpoint. Pressure was controlled manually rather than quantified instrumentally. The bowel was returned to the abdominal cavity and the abdominal wall closed in layers. Postoperative monitoring covered activity, food intake, bowel function, body weight and signs of complications. Intact controls remained unmanipulated baseline references and underwent neither surgery nor vehicle gavage.

Beclomethasone dipropionate raw substance (USP/Ph. Eur. pharmacopoeial grade) was officially imported, certified and distributed by Grand Pharm Trade (Tashkent, Uzbekistan), with State Registration No. DV/X 08421/09/24 and Batch/Lot No. BC-20240812-UZ. The substance was stored sealed at 2–8 °C, protected from light, in accordance with the manufacturer storage instructions. Each morning, a fresh suspension was prepared in aqueous 0.5% sodium carboxymethylcellulose (CMC) at 0.01 mg/mL. Suspensions were kept at 20–22 °C and used within 2 hours of preparation. A rounded-tip stainless-steel oral gavage needle delivered 5.0 mL/kg body weight, corresponding to 0.05 mg/kg, once daily at a consistent time for 14 consecutive days from POD 14. Dosing volume was adjusted to body weight. No vehicle-only gavage control arm was included. Our study records identify the distributor, registration and batch, but do not specify the original manufacturer or a manufacturer catalog number.

Drug administration began on POD 14 to allow a postoperative interval for adhesion development. No intermediate diagnostic laparotomy was performed, to avoid additional surgical trauma before dosing. Terminal macroscopic inspection confirmed adhesion presence, but does not directly verify its presence or severity in each animal at POD 14. Numerical adhesion grading was not recorded. Thyroid tissue was sampled 24 hours after the final dose, with time-matched intact controls. Euthanasia was performed using sodium pentobarbital overdose (150 mg/kg, intraperitoneally), followed by cervical dislocation.

Histology and morphometry

Thyroid tissue was dissected, fixed in 10% neutral formalin, embedded in paraffin and sectioned at 4–5 µm for H&E staining. Assessment covered follicular organization, colloid distribution, capsule appearance, interfollicular tissue and perivascular changes. Retained morphometric summaries comprise follicular diameter, cross-sectional area, stromal proportion and vascular density. The original mean ± SEM notation is reproduced for traceability, but the underlying experimental unit, field-aggregation procedure and individual-animal values cannot be verified. The reported SEM values therefore cannot be used to estimate animal-level variability or confidence intervals.

Histochemical staining

doi:10.22034/ijp.2026.2089875.3724

Table 1. Reported positive areas in selected histochemical image regions

Stain and measure	12 months Control	12 months Experimental	18 months Control	18 months Experimental
Van Gieson positive area, %	16.2	36.8	21.4	38.8
Alcian blue positive area, %	4.6	14.5	4.7	13.6

The parent study described Van Gieson staining with hematoxylin, picric acid and acid fuchsin, followed by dehydration, clearing and mounting, and Alcian blue staining at pH 2.5. The dissertation describes outlining tissue regions on micrographs and calculating positive area as the stained area divided by the outlined tissue area, multiplied by 100. For the present report, the retained percentages were transcribed rather than generated by a new image analysis. The available records do not establish a fixed number of ROIs per section, the number of contributing sections or animals, independent blinded assessment, or the image-to-animal mapping. Numerical stain thresholds, calibration values and segmentation settings could not be verified. Our intended sampling approach comprised five ROIs per tissue section; however, the retained records do not verify its implementation or completeness for the reported summaries. This planned number is not used to reconstruct actual ROI totals, and independent blinded assessment is not asserted. Table 1 presents archived selected-region percentages, not animal-level group means. Alcian blue positivity is reported as stain-positive area without assigning a specific biochemical substrate.

Ki-67 immunohistochemistry

Ki-67 immunohistochemistry was performed on 4–5 µm paraffin-embedded thyroid sections using a rabbit monoclonal anti-Ki-67 antibody (clone SP6; Abcam, catalogue ab16667; dilution 1:200), reported as validated for reactivity with rat tissue. Following deparaffinization and rehydration, heat-induced epitope retrieval was performed in 10 mM sodium citrate buffer (pH 6.0) at 95°C for 20 minutes. Rat spleen sections served as positive tissue controls; omission of the primary antibody served as the negative control. A secondary detection system and DAB chromogen were used, followed by hematoxylin counterstaining.

The dissertation reports Ki-67 assessment on DAB-stained images at ×200 magnification using QuPath version 0.5.1 (15), with selection of several microscopic fields per preparation and assessment primarily of follicular epithelial cells. The archived age/arm entries represent pooled positive and negative cell counts across selected ROIs in the analyzed images, rather than counts from a single image or a single ROI. Pooling was recorded at the age/arm level, but a recoverable image-by-image, section-by-section or animal-by-animal count ledger is unavailable. The exact number and area of the contributing ROIs and the number of represented sections and animals cannot be established. Although the intended target was follicular epithelium, complete exclusion of endothelial cells, fibroblasts and other interstitial elements cannot be audited from the pooled counts alone. We intended to select five ROIs per tissue section. This describes the sampling plan, not a verified count of regions actually analyzed. Compliance with that plan, independent blinded assessment and uniform numerical detection thresholds cannot be confirmed from the retained records. The present analysis transcribed these pooled summaries without new cell detection or reconstruction of missing sampling records.

For this report, total cells denotes the sum of the archived Ki-67-positive and Ki-67-negative cell counts pooled across selected ROIs within each age/arm stratum. The arithmetic positive fraction was calculated as 100 × pooled positive / (pooled positive + pooled negative). It is a cell-count-weighted fraction for the retained selected regions, not a mean of individual-animal proliferation indices or a whole-gland count. The fractions in Table 2 were recalculated directly from the counts rather than copied from the dissertation percentages. Pooling does not establish that all surviving animals contributed, and the known cohort sizes were not used as quantitative denominators. Neither cells nor images were treated as independent animal replicates.

Analysis

The present analysis used the dissertation and retained summary measurements as secondary source material. The original experimental procedures are described above as procedures of the parent study; the work performed for this report comprised transcription of the available summaries, checking arithmetic differences and recalculating fractions from the pooled selected-ROI Ki-67 counts. No new tissue processing, ROI sampling or image quantification was undertaken for this analysis. The parent-study surviving cohort comprised 64 animals: 20 controls and 44 experimental animals, distributed as 10 controls and 23 experimental animals at 12 months and 10 controls and 21 experimental animals at 18 months. These are cohort counts; the exact numbers contributing to each archived quantitative endpoint remain unverified. No ROI total was estimated by multiplying the survivor counts by the planned five ROIs per section, because the number of sections and actual sampling coverage are unknown. Morphometric mean ± SEM entries retain the source notation, but their experimental unit and aggregation cannot be reconstructed. No inferential tests, confidence intervals or age-by-exposure analyses were performed. Cells and image fields were not treated as independent animal replicates (16).

Table 2. Pooled selected-ROI Ki-67 cell counts and recalculated arithmetic fractions

Age and arm	Positive cells	Negative cells	Total cells	Positive fraction %
12 months, control	42	221	263	15.97
12 months, experimental	4	51	55	7.27
18 months, control	30	143	173	17.34
18 months, experimental	4	43	47	8.51

doi:10.22034/ijp.2026.2089875.3724

Table 3. Initial allocation and recorded deaths

Arm	Age months	Allocated n	Deaths n	Death POD	Survivors n
Intact control	12	10	0	—	10
Combined exposure	12	25	2	3, 5	23
Intact control	18	10	0	—	10
Combined exposure	18	25	4	2, 4, 6, 8	21

RESULTS

Allocation and available outcomes

Of 70 allocated animals, 20 were intact controls and 50 were experimental animals. Two 12-month experimental rats died on PODs 3 and 5, and four 18-month experimental rats on PODs 2, 4, 6 and 8, all before gavage began on POD 14. Reduced locomotor activity and transient piloerection preceded death. Gross post-mortem inspection showed no intestinal perforation, suture dehiscence, mechanical bowel obstruction or generalized peritonitis. Surgical stress and individual vulnerability were suspected, without definitive individual causes established. No other animals were excluded from the surviving cohorts. All 64 survivors completed the study and histological/immunohistochemical evaluation (Table 3 and Figure 1). Archived quantitative outputs consist of grouped summaries and selected-region counts without individual-animal tracking, preventing independent animal-level reanalysis.

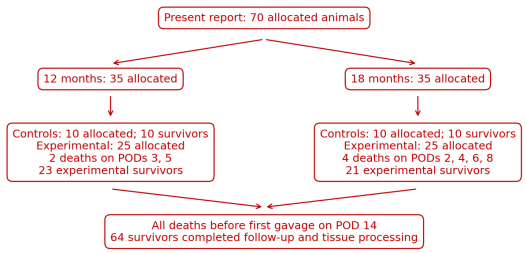


Fig 1. Animal flow in the present report

POD, postoperative day. All six deaths occurred before dosing began on POD 14. Gross necropsy showed no intestinal perforation or generalized peritonitis; postoperative complications or surgical stress were suspected. All survivors completed follow-up and underwent histological and immunohistochemical processing. Survivor counts do not establish the animal-level denominators underlying the retained numerical summaries. The separate ginger arm is outside this report.

Follicular morphology and morphometry

Control sections showed round or oval follicles containing colloid and lined predominantly by cuboidal follicular cells. Following the combined experimental protocol, the descriptive histology identified uneven capsular thickening, perivascular edema, connective-tissue expansion and regional variation in follicular size and colloid content. These findings were qualitative; frequencies and blinded severity scores were not available.

Group summaries showed small absolute differences in average follicular dimensions (Table 4). Experimental minus control differences in diameter were 0.5 µm at 12 months and 1.8 µm at 18 months; the corresponding area differences were 19 and 80 µm^2. Stromal proportions differed by 1.2 and 0.2 percentage points, respectively. The available summary values do not establish statistically significant follicular enlargement or an age-dependent treatment response.

Entries reproduce retained mean ± SEM summaries; their animal-level derivation cannot be verified. Experimental denotes combined serosal injury, postoperative recovery, gavage, vehicle and beclomethasone exposure. Survivor counts are given in Table 3 and must not be treated as validated denominators for these summaries. No inferential comparison or animal-level variability estimate is presented.

Stromal staining

Reported Van Gieson-positive areas were higher in the selected experimental image regions than in the corresponding control regions (Table 1). The differences were 20.6 percentage points at 12 months and 17.4 percentage points at 18 months. Alcian blue-positive area measurements were also higher in the experimental regions. These selected-ROI values describe the selected tissue regions and cannot be interpreted as whole-gland collagen content or animal-level means.

Values reproduce archived selected-region positive-area percentages. The numbers of contributing images, ROIs, sections and animals, and their aggregation, could not be established. These values are not verified animal-level group means, and implementation of the intended five-ROI-per-section plan cannot be verified. The outlined tissue-area denominators cannot be established as equivalent to the stromal-proportion denominator in Table 4.

Ki-67 labeling

The archived pooled selected-ROI Ki-67 counts comprised 42 positive and 221 negative cells in the 12-month control stratum, 4 and 51 in the corresponding experimental stratum, 30 and 143 in the 18-month control stratum, and 4 and 43 in the corresponding experimental stratum (Table 2). The resulting totals are 263, 55, 173 and 47, with arithmetic positive fractions of 15.97%, 7.27%, 17.34% and 8.51%, respectively. These

Table 4. Thyroid morphometric summary measurements

Parameter	12 months Control	12 months Experimental	18 months Control	18 months Experimental
Follicular diameter, µm	66.2 ± 3.1	66.7 ± 3.3	67.3 ± 3.4	69.1 ± 3.6
Follicular area, µm^2	3194 ± 147	3213 ± 151	3261 ± 157	3341 ± 161
Stromal proportion, %	11.7 ± 0.4	12.9 ± 0.4	13.2 ± 0.6	13.4 ± 0.7
Vascular density, n/mm^2	16.7 ± 0.7	17.6 ± 0.8	18.4 ± 0.8	18.5 ± 1.0

entries are pooled across selected ROIs within each stratum, not counts per image or per animal. The experimental entries have lower numerical fractions, but comparable sampled tissue areas, cell composition and sampling effort cannot be established. The larger experimental cohort sizes do not imply that more tissue area or more ROIs contributed to the retained cell counts. The archived summaries provide no verified measure of sampling coverage with which to explain the smaller experimental totals. The totals include both positive and negative cells; consequently, lower Ki-67 positivity alone does not explain their smaller size. No biological explanation for this difference in total counts is established by the retained data.

Total cells = pooled positive + pooled negative counts across selected ROIs within the stated age/arm stratum; fraction = 100 × pooled positive/total, rounded to two decimals. These are archived selected-region totals, not whole-gland counts or verified totals covering every surviving animal. The numbers of contributing images, ROIs, sections and animals, the tissue areas sampled and complete exclusion of non-follicular cells cannot be verified. The fractions are descriptive pooled-cell summaries, not animal-level or follicular-cell-specific proliferation indices. The intended five ROIs per section must not be treated as the observed sampling denominator.

DISCUSSION

This exploratory analysis of a larger experimental project documents a consistent descriptive pattern in the retained summaries: selected experimental regions had higher Van Gieson- and Alcian blue-positive area percentages at both ages, whereas reported mean follicular dimensions differed little numerically. Archived pooled selected-ROI Ki-67 counts yielded lower arithmetic positive fractions in the experimental strata, although the contributing sampling units and cell composition remain unverified. The contribution is a description of these archived observations and the traceability gaps that must be addressed before testing them at the animal level.

Glucocorticoid-related suppression of TSH provides a biological reason to examine thyroid responses during steroid exposure (1). The adult-rat dexamethasone study by El Shaer and Elkelany also demonstrates the relevance of combining tissue morphology with biochemical assessment (2). However, the present experiment used a different glucocorticoid and dose in animals subjected to prior surgery. No circulating TSH, free thyroxine or triiodothyronine measurements were available. Thus, neither clinical hypothyroidism nor preservation of normal hormone secretion can be inferred from the reported histology. Thyroid-hormone administration has itself produced follicular and ultrastructural changes in rats, illustrating that morphology can respond to altered endocrine feedback (17). In a separate carbamazepine model, Akorede and colleagues measured thyroid hormone concentrations alongside other toxicological outcomes (18). These different exposure models support pairing histology with endocrine measurements; their findings cannot be transferred directly to the present beclomethasone protocol. Pharmacological suppression of TSH does not necessarily produce clinically evident central hypothyroidism, reinforcing the need to distinguish endocrine regulation from structural injury (19). Thyroid weight and other endocrine endpoints were also unavailable for this analysis.

There were no sham-operated, injury-only, vehicle-only or beclomethasone-only comparator arms in the present analysis. Intact controls provide an unmanipulated baseline comparison, not a validated physiological reference interval. They cannot separate serosal injury, adhesion formation, postoperative recovery, repeated gavage, vehicle and drug exposure. Adhesion biology involves inflammatory and reparative processes (4, 5), but neither the specific cause of the thyroid observations nor anti-adhesion efficacy can be determined here. Collagen staining in selected regions does not establish whole-gland fibrosis, a causal pathway or progressive organ dysfunction (20). The exploratory design supports planning additional comparator arms rather than attributing the observations specifically to beclomethasone.

The scale of measurement remains an important limitation. Van Gieson-positive area summaries exceed the reported general morphometric stromal proportions, including in controls. Their sampling and denominator equivalence cannot be verified, so these endpoints cannot be treated as interchangeable measurements of the same compartment. The dissertation describes outlined image regions, but the available material does not establish the full selection or aggregation procedure underlying Table 1. Color deconvolution can separate stain signals (21), while optical conditions and spectral assumptions can introduce measurement error (22); these general methodological principles do not verify the undocumented settings of the archived analysis. The percentages therefore describe the retained selected regions without establishing whole-gland fibrosis or a substrate-specific biochemical change.

Ki-67 provides information about cell-cycle-associated labeling, but its expression depends on cell-cycle regulation and cellular state (9, 10). The lower arithmetic fractions describe only the archived pooled selected-ROI counts. Their denominators include positive and negative cells, and reduced expression cannot by itself account for a smaller total number of counted cells. Undocumented sampling effort and incomplete verification of cell types prevent interpretation as a comparative follicular epithelial response. Differences in tissue preservation, the amount of evaluable epithelium, region selection or cell detection are possible explanations for unequal count totals, but the archive contains no image-quality scores, sampled-area measurements or inclusion/exclusion logs with which to test them. Better preservation in controls or atrophy in experimental tissue is therefore not established as the cause. Surgery, postoperative stress and drug exposure cannot be assigned as causes of the smaller totals from these records. They do not demonstrate increased apoptosis, irreversible cell loss or diminished long-term regenerative capacity. Establishing such interpretations would require additional endpoints and animal-level measurements. QuPath facilitates region-based cell detection and classification (15), but software use alone does not establish biological replication. Application-specific antibody validation and appropriate tissue controls are essential to the interpretation of immunohistochemistry (23, 24). The established use of Ki-67 as a growth-fraction marker (25) and its broader roles in chromatin organization (26) further caution against equating reduced labeling with cell death. Standardization work in breast cancer emphasizes preanalytical handling and calibrated scoring (27); its disease-specific clinical cutoffs cannot be transferred to non-neoplastic rat thyroid tissue. Heat-induced antigen retrieval can alter epitope detection in formalin-fixed tissue (28), making comparable processing across groups important.

The numerical age comparisons were not uniform. Older experimental regions had a higher collagen-positive area than younger regions, but their Alcian blue-positive area was lower and their count-based Ki-67 fraction was higher. Differences in baseline values also varied by endpoint. These observations do not support a general claim that all thyroid alterations were more severe at 18 months. A formal age interaction requires animal-level measurements and a design capable of distinguishing age from other differences between strata.

The principal limitations are missing individual-animal measurements, unresolved image-to-animal linkage and incomplete numerical segmentation and aggregation records. Although the Ki-67 counts are pooled selected-ROI totals within each age/arm stratum, the exact contributing images, sections and animals, the consistency of sampled areas and complete exclusion of non-follicular cells remain unverified. Our intended sampling approach comprised five ROIs per section, but the available records do not establish its execution for each specimen. Differences between the sampling plan and the recoverable observations cannot be quantified. Differential mortality (2/25 and 4/25 experimental animals, versus no control deaths) may introduce survivor bias. Because all deaths occurred on PODs 2–8, before gavage began on POD 14, they cannot be attributed to the administered beclomethasone or vehicle; their precise postoperative causes remain uncertain. Adhesions were evaluated macroscopically at termination. No intermediate diagnostic laparotomy was undertaken, to avoid additional surgical trauma before dosing, so adhesion presence or severity at POD 14 was not directly verified in each animal. No numerical severity dataset is available. Intact controls were unmanipulated; the absence of a vehicle-only gavage group and other procedural comparator arms prevents separation of handling, surgery, vehicle and drug effects. The pre-dosing timing of the deaths does not establish that mortality had no influence on the composition of the surviving cohorts. The absence of a recoverable sampling ledger also prevents assessment of selection within the archived images. Summary SEM values cannot substitute for such data. ARRIVE emphasizes transparent reporting of experimental units, exclusions and bias-reduction methods (13, 14, 16); cells and fields are nested observations rather than independent biological replicates (29, 30).

A follow-up study should pair each thyroid specimen with an animal identifier, apply prespecified and blinded sampling, report calibrated images and retain the underlying cell-classification outputs. Time-matched sham-operated, untreated-adhesion and drug-only groups would help distinguish the exposures. Measurements of circulating TSH and free T4 would then allow structural observations to be tested against endocrine function. The current findings are useful for defining those questions, but their reproducibility and functional significance remain to be established.

CONCLUSION

The archived summaries document higher Van Gieson- and Alcian blue-positive area percentages in selected experimental thyroid regions at both ages, alongside small numerical differences in reported follicular dimensions. The pooled selected-ROI Ki-67 counts yield lower arithmetic positive fractions in the experimental strata, but undocumented sampling and unverified cell composition prevent a biological between-group interpretation. These findings identify a descriptive staining pattern for further investigation after combined serosal injury and beclomethasone exposure. Confirmation requires traceable animal-level measurements, documented sampling, separate procedural and drug comparator groups, and thyroid hormone measurements.

ABBREVIATIONS

CMC: carboxymethylcellulose
DAB: 3,3′-diaminobenzidine
H&E: hematoxylin and eosin
ROI: region of interest
SEM: standard error of the mean
TSH: thyroid-stimulating hormone.

Funding

This research received no funding.

Conflict of interest

The authors declare no financial or nonfinancial conflicts of interest.

Data Availability

The summary measurements and archived pooled selected-ROI cell counts transcribed for this report are provided in Tables 1–4. The Ki-67 archive retains pooled positive and negative counts for each age/arm stratum rather than a complete set of individual-image or individual-animal records. The source dissertation contains illustrative micrographs and descriptions of the original methods, but it does not supply a verifiable mapping from each quantitative entry to its contributing images, sections and animals. The current analysis recalculated Ki-67 positive fractions from the reported pooled positive and negative counts; it did not reconstruct the original image-analysis dataset. Animal-level measurements, original QuPath project files or cell-level exports, and a complete sampling ledger were unavailable for this analysis.

Ethics Approval

The animal study was approved by the Ethics Committee of Bukhara State Medical Institute (protocol No. 46, dated 23 May 2025).

Authors' Contributions

Conceptualization: B.A. Kibriev and M.O. Umbarov; Methodology, Investigation, and Data Curation: B.A. Kibriev; Writing – Original Draft: B.A. Kibriev; Writing – Review & Editing: M.O. Umbarov, R.B. Mengliyeva, and N.A. Ergashev. B.A. Kibriev performed morphological and morphometric assessment. M.O. Umbarov and R.B. Mengliyeva reviewed the literature. All four authors contributed to interpretation of the findings; N.A. Ergashev also critically revised the manuscript for important intellectual content.

Acknowledgments

This article derives from B.A. Kibriev's doctoral dissertation on thyroid morphology following hormonal treatment of experimental intestinal scar and adhesion formation.

Declaration of AI Use

ChatGPT (OpenAI) was used to assist with manuscript drafting and language editing. The authors reviewed and verified the final manuscript and take responsibility for its accuracy and integrity.

REFERENCES

1. Wilber JF, Utiger RD. The effect of glucocorticoids on thyrotropin secretion. J Clin Invest. 1969;48:2096-2103. [DOI:10.1172/JCI106176] [PMCID:PMC297463] [PMID:4980930]

2. El Shaer DF, Elkelany MM. Adverse effect of dexamethasone on the thyroid gland of adult male albino rat and the possible protective role of curcumin: Histological, immunohistochemical and biochemical study. Egypt J Histol. 2023;46:619-634. [DOI:10.21608/ejh.2022.110057.1602]

3. Alkemade A, Unmehopa UA, Wiersinga WM, Swaab DF, Fliers E. Glucocorticoids decrease thyrotropin-releasing hormone messenger ribonucleic acid expression in the paraventricular nucleus of the human hypothalamus. J Clin Endocrinol Metab. 2005;90(1):323-327. [DOI:10.1210/jc.2004-1430] [PMID:15509645]

4. Ito T, Shintani Y, Fields L, Shiraishi M, Podaru MN, Kainuma S, et al. Cell barrier function of resident peritoneal macrophages in post-operative adhesions. Nat Commun. 2021;12:2232. [DOI:10.1038/s41467-021-22536-y] [PMCID:PMC8046819] [PMID:33854051]

5. Li L, Hirao H, Honda M, Adawy A, Pan C, Fujiwara Y, et al. Preventive role of CD163-positive macrophages in postoperative peritoneal adhesions. Inflamm Regen. 2025;45:26. [DOI:10.1186/s41232-025-00392-3] [PMCID:PMC12355886] [PMID:40817081]

6. Fischer A, Koopmans T, Ramesh P, Christ S, Strunz M, Wannemacher J, et al. Post-surgical adhesions are triggered by calcium-dependent membrane bridges between mesothelial surfaces. Nat Commun. 2020;11:3068. [DOI:10.1038/s41467-020-16893-3] [PMCID:PMC7299976] [PMID:32555155]

7. Tsai JM, Sinha R, Seita J, Fernhoff N, Christ S, Koopmans T, et al. Surgical adhesions in mice are derived from mesothelial cells and can be targeted by antibodies against mesothelial markers. Sci Transl Med. 2018;10(469):6735. [DOI:10.1126/scitranslmed.aan6735] [PMID:30487249]

8. Elrod J, Heuer A, Knopf J, Schoen J, Schönfeld L, Trochimiuk M, et al. Neutrophil extracellular traps and DNases orchestrate formation of peritoneal adhesions. iScience. 2023;26(12):108289. [DOI:10.1016/j.isci.2023.108289] [PMCID:PMC10682263] [PMID:38034352]

9. Uxa S, Castillo-Binder P, Kohler R, Stangner K, Müller GA, Engeland K. Ki-67 gene expression. Cell Death Differ. 2021;28:3357-3370. [DOI:10.1038/s41418-021-00823-x] [PMCID:PMC8629999] [PMID:34183782]

10. Miller I, Min M, Yang C, Tian C, Gookin S, Carter D, et al. Ki67 is a graded rather than a binary marker of proliferation versus quiescence. Cell Rep. 2018;24:1105-1112. [DOI:10.1016/j.celrep.2018.06.110] [PMCID:PMC6108547] [PMID:30067968]

11. Sobecki M, Mrouj K, Camasses A, Parisis N, Nicolas E, Llères D, et al. The cell proliferation antigen Ki-67 organises heterochromatin. eLife. 2016;5:e13722. [DOI:10.7554/eLife.13722] [PMCID:PMC4841783] [PMID:26949251]

12. Cuylen S, Blaukopf C, Politi AZ, Müller-Reichert T, Neumann B, Poser I, et al. Ki-67 acts as a biological surfactant to disperse mitotic chromosomes. Nature. 2016;535(7611):308-312. [DOI:10.1038/nature18610] [PMCID:PMC4947524] [PMID:27362226]

13. Percie du Sert N, Hurst V, Ahluwalia A, Alam S, Avey MT, Baker M, et al. The ARRIVE guidelines 2.0: Updated guidelines for reporting animal research. PLoS Biol. 2020;18:e3000410. [DOI:10.1371/journal.pbio.3000410] [PMCID:PMC7360023] [PMID:32663219]

14. Percie du Sert N, Ahluwalia A, Alam S, Avey MT, Baker M, Browne WJ, et al. Reporting animal research: Explanation and elaboration for the ARRIVE guidelines 2.0. PLoS Biol. 2020;18(7):e3000411. [DOI:10.1371/journal.pbio.3000411] [PMCID:PMC7360025] [PMID:32663221]

15. Bankhead P, Loughrey MB, Fernández JA, Dombrowski Y, McArt DG, Dunne PD, et al. QuPath: Open source software for digital pathology image analysis. Sci Rep. 2017;7:16878. [DOI:10.1038/s41598-017-17204-5] [PMCID:PMC5715110] [PMID:29203879]

16. Lazic SE, Clarke-Williams CJ, Munafò MR. What exactly is N in cell culture and animal experiments?. PLoS Biol. 2018;16(4). [DOI:10.1371/journal.pbio.2005282] [PMCID:PMC5902037] [PMID:29617358]

17. Ali Rajab NM, Ukropina M, Cakic-Milosevic M. Histological and ultrastructural alterations of rat thyroid gland after short-term treatment with high doses of thyroid hormones. Saudi J Biol Sci. 2017;24(6):1117-1125. [DOI:10.1016/j.sjbs.2015.05.006] [PMCID:PMC5562382] [PMID:28855802]

18. Akorede GJ, Ambali SF, Olatunji AO, Aremu A, Ahmed AO, Basiru A, et al. Vitamin C protects against blood and thyroid toxicities induced by the chronic use of carbamazepine in rats. Iran J Toxicol. 2023;17(2):147-156. [DOI:10.32598/IJT.17.2.1080.1]

19. Haugen BR. Drugs that suppress TSH or cause central hypothyroidism. Best Pract Res Clin Endocrinol Metab. 2009;23(6):793-800. [DOI:10.1016/j.beem.2009.08.003] [PMCID:PMC2784889] [PMID:19942154]

20. Wynn TA, Ramalingam TR. Mechanisms of fibrosis: therapeutic translation for fibrotic disease. Nat Med. 2012;18(7):1028-1040. [DOI:10.1038/nm.2807] [PMCID:PMC3405917] [PMID:22772564]

21. Ruifrok AC, Johnston DA. Quantification of histochemical staining by color deconvolution. Anal Quant Cytol Histol. 2001;23(4):291-299. [PMID:11531144]

22. Haub P, Meckel T. A model based survey of colour deconvolution in diagnostic brightfield microscopy: Error estimation and spectral consideration. Sci Rep. 2015;5:12096. [DOI:10.1038/srep12096] [PMCID:PMC4519787] [PMID:26223691]

23. Uhlen M, Bandrowski A, Carr S, Edwards A, Ellenberg J, Lundberg E, et al. A proposal for validation of antibodies. Nat Methods. 2016;13(10):823-827. [DOI:10.1038/nmeth.3995] [PMCID:PMC10335836] [PMID:27595404]

24. Hewitt SM, Baskin DG, Frevert CW, Stahl WL, Rosa-Molinar E. Controls for immunohistochemistry: the Histochemical Society's standards of practice for validation of immunohistochemical assays. J Histochem Cytochem. 2014;62(10):693-697. [DOI:10.1369/0022155414545224] [PMCID:PMC4212362] [PMID:25023613]

25. Scholzen T, Gerdes J. The Ki-67 protein: from the known and the unknown. J Cell Physiol. 2000;182(3):311-322. [DOI:10.1002/(sici)1097-4652(200003)182:3<311::aid-jcp1>3.0.co;2-9] [PMID:10653597]

26. Sun X, Kaufman PD. Ki-67: more than a proliferation marker. Chromosoma. 2018;127(2):175-186. [DOI:10.1007/s00412-018-0659-8] [PMCID:PMC5945335] [PMID:29322240]

27. Nielsen TO, Leung SCY, Rimm DL, Dodson A, Acs B, Badve S, et al. Assessment of Ki67 in Breast Cancer: Updated Recommendations From the International Ki67 in Breast Cancer Working Group. J Natl Cancer Inst. 2021;113(7):808-819. [DOI:10.1093/jnci/djaa201] [PMCID:PMC8487652] [PMID:33369635]

28. Shi SR, Key ME, Kalra KL. Antigen retrieval in formalin-fixed, paraffin-embedded tissues: an enhancement method for immunohistochemical staining based on microwave oven heating of tissue sections. J Histochem Cytochem. 1991;39(6):741-748. [DOI:10.1177/39.6.1709656] [PMID:1709656]

29. Lazic SE. The problem of pseudoreplication in neuroscientific studies: is it affecting your analysis?. BMC Neurosci. 2010;11:5. [DOI:10.1186/1471-2202-11-5] [PMCID:PMC2817684] [PMID:20074371]

30. Vaux DL, Fidler F, Cumming G. Replicates and repeats--what is the difference and is it significant? A brief discussion of statistics and experimental design. EMBO Rep. 2012;13(4):291-296. [DOI:10.1038/embor.2012.36] [PMCID:PMC3321166] [PMID:22421999]